Pergamon

Journal of Structural Geology, Vol. 16, No. 10, pp. 1417 to 1429, 1994

0191-8141/94 $7.00+0.00

0191-8141(94)E0006-K

Fluctuation in porosity and fluid pressure during hydrothermal events: textural evidence in the Emuford District, Australia

A.-M. BOULLIER and B. CHAROY*

Centre de Recherches Pétrographiques et Géochimiques, BP 20, 54501 Vandoeuvre-lès-Nancy, France

and

P. J. POLLARD

Department of Geology and Key Centre in Economic Geology, James Cook University, Townsville, Queensland 4811, Australia

(*Received* 14 *May* 1992; *accepted in revised form* 4 *January* 1994)

Abstract—The Upper Paleozoic granites of the Emu Suite, north Queensland, show varying degrees of alteration. The petrographic and microstructural survey of albite-rich zones reveals the spatial overprint of hydrothermal events which are more correlated with changes in physical conditions (permeability, fluid pressure and flow regime) rather than with chemical variations of the percolating fluids. The sequence of alteration events chronologically comprises: (1) *in situ* substitution of primary microline to chessboard albite; (2) dissolution of magmatic quartz resulting in the formation of interconnected vugs; (3) formation of concentric cracks around some vugs; (4) infilling of vugs; and (5) development of a dense system of closely spaced, sheeted veinlets by a crack–seal process. The first two stages indicate an increase of the global permeability of the albite zones (chemically induced porosity), whereas the vug- and vein-filling stages indicate the reverse, resulting in an increase of fluid pressure from nearly hydrostatic to nearly lithostatic values (mechanically induced porosity). This contrast is discussed from micro- and mesostructural arguments and from results of a fluid inclusion investigation; it is explained by the progressive focusing of the circulating fluids via grain boundaries, then vugs, and through tapping by late-stage microfracturing.

INTRODUCTION

HYDROTHERMAL alteration in granitic bodies is a very common feature. High-temperature feldspathic alteration (microcline, albite) and greisenization (phyllic alteration) are very common, especially in relation with Sn and W (but also Mo and Cu) mineralizations. Such alteration may be pervasive and incipient or fracture-controlled. Substantial variations in the type of alteration may be controlled by continual changes in fluid chemistry (alkali cation activity ratios and/or salinity–acidity relationships) through exchange with host rocks. For example, greisenization requires relatively acid fluids (hydrogen metasomatism of Hemley *et al.*, 1980, Burt 1981) whereas feldspathic alteration will be produced by weakly alkaline fluids (Orville 1963). Change in the nature or abundance of complexing ligands (B, Cl or F) may be also determinant in the type of feldspathic alteration (Pollard *et al.* 1987). Together with chemical evolution with time, change in ambiant pressure is also a dominant parameter to monitor the type and/or style of alteration and the key role of fluid pressure during processes of ore deposition is abundantly outlined in the economic geological literature (Guilbert & Park 1986). For example, albitization of K-feldspar will be promoted by a drop in pressure (Orville 1963). Fluid circulation is a normal consequence of the thermal disequilibrium induced by rising and emplacement of magmas high in the crust into fluid-bearing host rocks; convective heat flux becomes dominant over conductive heat flux (Norton & Knight 1977). Isotherms around the intrusion will govern the geometry of pathlines along which fluids will be able to flow. Such a circulation may be initiated through hydraulic fracturing up to extensive mechanical brecciation induced by retrograde boiling, i.e. the explosive release of volatiles boiled off a residual crystallizing magma at low pressure (shallow depth). This was well documented in numerous porphyry copper systems (Brimhall 1977, Burnham 1979). Migration of fluids has to be submitted to the fluid potential field (pressure gradient) induced by the thermal disequilibrium and upward expansion of the magma intrusion, i.e. the regional or local stress field.

Such aspects of fluid mobility also interested structural scientists (Fyfe *et al.* 1978, Etheridge *et al.* 1984, Cox *et al.* 1986, 1991, Titley 1990). Fluid circulation is confined to the permeable, mainly fractured, zones above the pluton (Norton & Knapp 1977, Norton & Knight 1977). Permeability of a given rock describes the capacity of that rock to transmit a fluid and is a measure of the relative ease of fluid flow across a pressure

*Also at: Ecole Nationale Supérieure de Géologie, BP 452, 54001, Nancy Cédex, France.

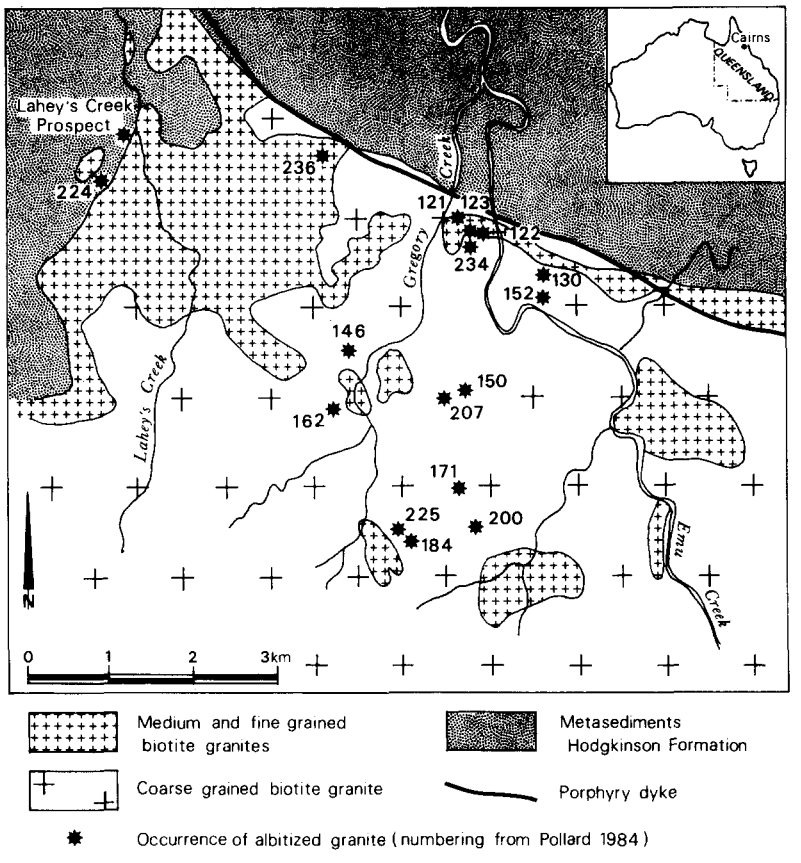

Fig. 1. Geological map of the Emuford district showing the location of the mineralized albite zones in the granite.

gradient. Permeability is the result of two different contributing effects: one primary (intrusive), depending of the nature of the rock itself and the other secondary (or induced), expressive of the geological history of the rock. At the same place, the permeability of a rock formation may be highly variable, mostly resulting from its tectonic history (hydraulic fracturing) but also from its reactive behaviour through solid(s)–fluid(s) reactions: reduction of grain size or dissolution. The porosity parameter (ratio of pore volume to total volume) is rarely approached in petrological or structural studies. The stress configuration is difficult to construct in a given volume of rock because of the telescoping influence of numerous internal and external parameters. The stress field (stress trajectories) will be only approached when a set of fractures is developed. The variation in local pressure may be abrupt (as stated before) or continuous, mainly by change from a nearly lithostatic to a nearly hydrostatic regime. However, fluctuation of fluid pressure rather than absolute magnitude may have important metallogenic consequences on the type and style of metal deposition and associated alteration, as recently demonstrated in some gold deposits (Sibson *et al.* 1988, Cox *et al.* 1991, Boullier & Robert 1992, Cathelineau *et al.* 1993). An identical approach is used in this paper on the example of localized tin-mineralized zones within granites of the Emuford district (northeast Queensland, Australia) in order to draw the link between the behaviour of the rocks during continuing hydrothermal alteration (replacement, dissolution, growth and deformation of initial and secondary minerals) and the qualitative fluctuations in physical parameters such as porosity and fluid pressure.

GEOLOGICAL SETTING

The Emuford district of the Herberton tin field is situated approximately 100 km southwest of Cairns in northeast Queensland (Fig. 1). Tin, tungsten and base metal mineralizations in this area are spatially and genetically related to the late-stage granites of the Emu Suite (Pollard 1988), a group of Upper Paleozoic, geochemically specialized, fluorine-rich biotite granites which intrude early Paleozoic metagreywackes and conglomerates of the Hodgkinson Formation gently folded during the Tasman orogeny (Blake & Smith 1970, Coney *et al.* 1990). Tin mineralization in the Emuford district is hosted both by the Hodgkinson metasediments and the Emu Suite granites. Within metasediments, cassiterite occurs mainly in swarms of: (1) quartz-tourmaline veins localized near the granite contact; and (2) quartz–chlorite–sulfide ± carbonate veins that crosscut the former. Both types of veins display tourmalinized or chloritized and/or silicified walls and have on average a NW–SE vertical orientation (Fig. 2) similar to the orientation of the fold axial planes defined in the Hodgkinson metasediments. These veins have not been studied in detail in the following study which is focused on the structures developed within the granites. Subdivisions in the Emu Suite granites are based largely on petrographic and textural grounds and include coarse-,

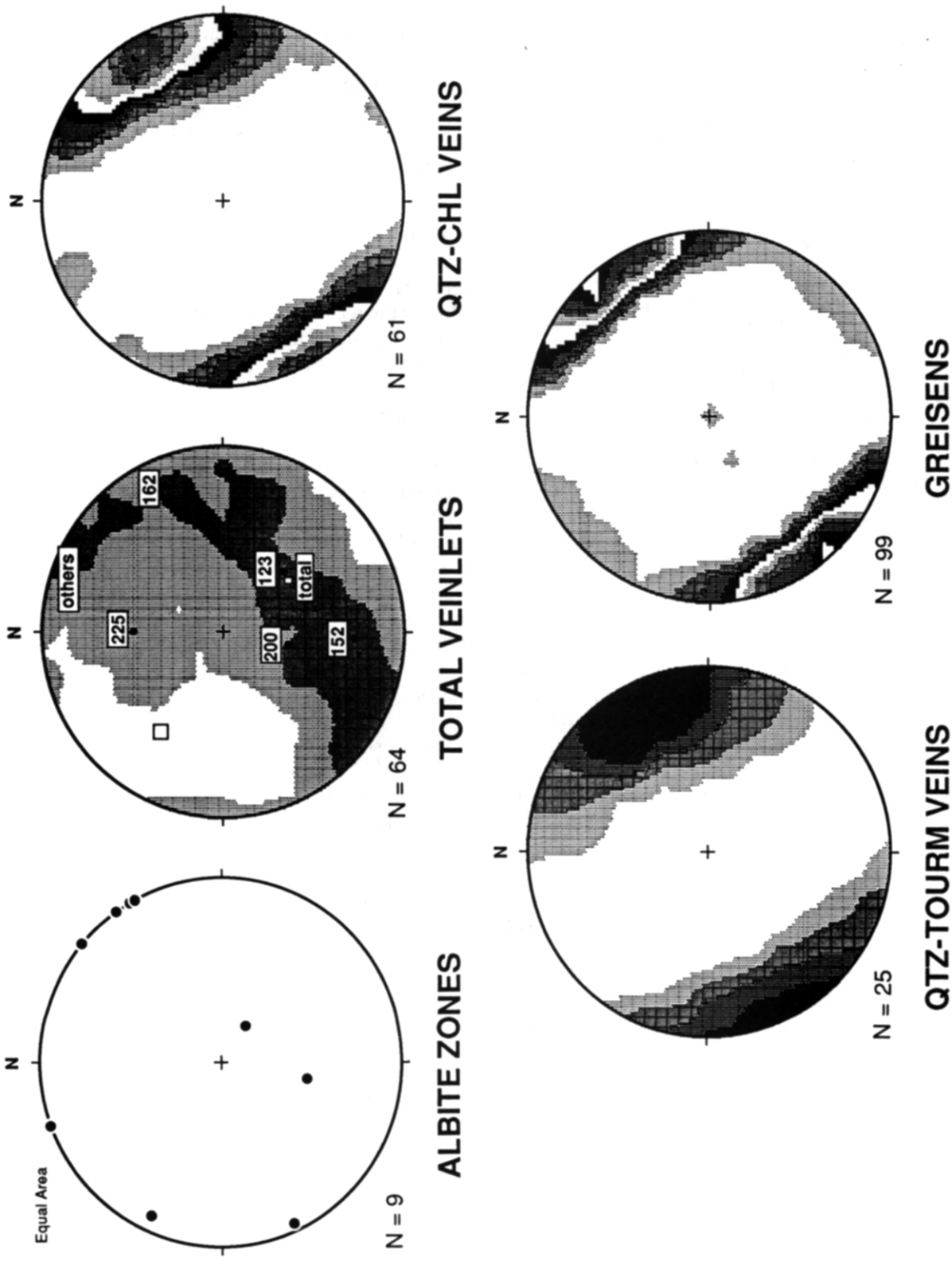

Fig. 2. Orientation of structures in the Emuford district: albite zones, swarms of quartz veinlets in the Emuford district, quartz–chlorite veins, quartz–tourmaline veins and greisens. Kamb contours (1% interval). Orientation data were handled with 'STEREONET' software (R. W. Allmendinger, Cornell University, Ithaca, New York). The stereogram of veinlets indicates the best-fit poles of the veinlets in the main sites as calculated with the same software.

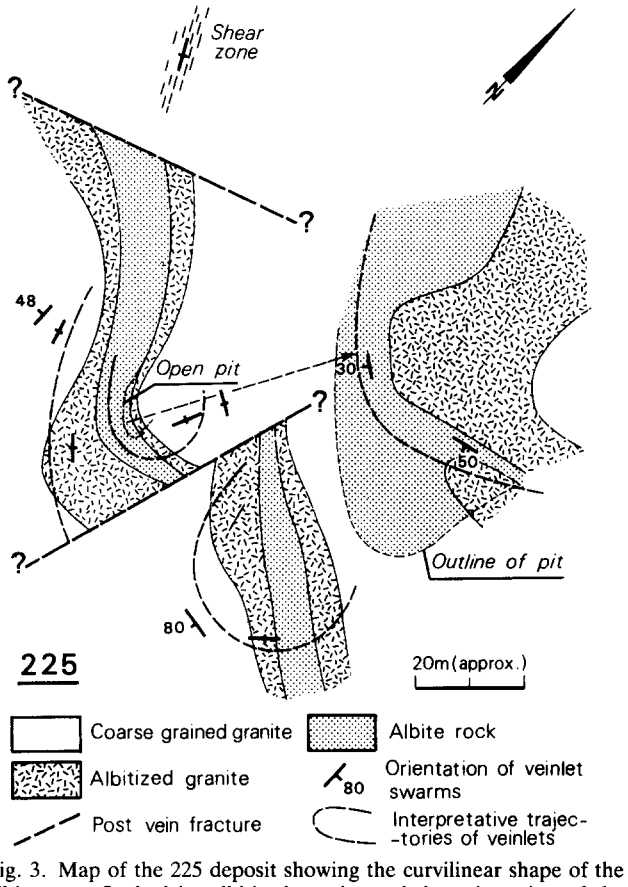

Fig. 3. Map of the 225 deposit showing the curvilinear shape of the albite zone flanked by albitized granite and the orientation of the veinlets.

medium- and fine-grained varieties. They are essentially composed of quartz, perthitic microcline, plagioclase (oligoclase–albite), biotite and minor topaz in the late, strongly fractionated varieties. The earliest stage of mineralization (wolframite, molybdenite and cassiterite) in the Emuford district is intimately related to the final stages of crystallization of the fine-grained granite varieties and pegmatites (Pollard 1984). Regardless of textural type, the granites are characterized by a widespread or localized development of secondary minerals (Pollard & Taylor 1986). Cassiterite mineralization in granites occurs: (1) in occasional albite zones with overprinted quartz-rich veinlet swarms (Fig. 2); and (2) in numerous NW–SE-trending fracture-controlled zones of greisenization. Cross-cutting relationships indicate that the albitized zones predate both quartz-rich veinlet swarms and the major stage of greisenization (Pollard & Taylor 1986, Charoy & Pollard 1989).

ZONES OF ALBITIZATION

The albitization process in the Emuford granite suite has been described by Pollard (1984) and Charoy & Pollard (1989). Zones of albitized rocks are mainly related in space to late-stage medium- and fine-grained, highly fractionated granites. They are apparently not localized by fractures, contrary to greisens which envelop rectilinear quartz veins. Albitized zones are narrow and often curved (Fig. 3). They consist of a central body of albite rock flanked by outer zones of albitized granite. Their orientation is not strongly defined on the stereogram but more than 50% of the albite zones examined in this survey are subvertical with a NW–SE strike, a direction which is close to that of the other hydrothermal structures (greisen-bordered veins, tourmaline- and chlorite-bearing veins) throughout the district (Fig. 2). Individual albite zones range from 0.5 to 10 m across, and extend for up to 100 m along strike (Fig. 3). A low-grade cassiterite mineralization is present and was actively (but artisanally) mined with the consequent nearly complete removal of the mineralized occurrences and the nearly complete obliteration of the spatial relations between the different zones.

Two deposits (225 and 152, Fig. 1) have been studied in great detail. This, together with numerous (and convergent) punctual observations in other deposits allowed the reconstruction of the chronological scenario of the mineralogical and structural events superimposed in this evolving hydrothermal system. The sequence in the progress of the albitization process includes three steps: unmodified granite, albitized granite and finally albite rock (Charoy & Pollard 1989). The unmodified granites are essentially composed of quartz, perthitic microcline, plagioclase (oligoclase to albite) and biotite. Coarsening of patch perthite is accompanied by some outward migration of exsolved albite as small new grains in crystallographic continuity with the perthite veins. This can change partly the feldspar grain boundaries (the 'swapped rim' of Parsons *et al.* 1988, see also Ramberg 1962, Peng 1970). A clear albite fringe rims the cloudy plagioclase crystals containing numerous inclusions of muscovite and fluorite.

The contact between the granite and the albitized granite is sharp even at the thin section scale and may cross-cut the alkali feldspar grains. Coarsening of perthite resulted in the complete replacement of the former alkali feldspar into chessboard albite (Smith 1974, Moore & Liou 1979). The general shape and crystallographic orientation (twin plane) of the original alkali feldspar have been preserved and are easily recognizable. At the same time, the former oligoclase was converted to albite, and biotite was completely dissolved and/or replaced by an assemblage of fluorite, muscovite, opaque minerals and carbonates. The albitized granite retains the major textural features of the parental granite: quartz is similar in shape and abundance to that in the granite.

In the albite rock, the granitic texture was partially obliterated. The shape of feldspars was roughly preserved but quartz was entirely dissolved which resulted in the formation of millimetric to centimetric vugs. Those vugs were subsequently filled by several generations of hydrothermal minerals. New albite occurs as an euhedral overgrowth on chessboard albite and albitic plagioclase, followed by turbid K-feldspar, minor golden muscovite, strongly zoned cassiterite, fluorite and quartz. New grown quartz occurs in two habits: as euhedral unstrained crystals often exhibiting Brazil twin (visible on basal sections with slightly uncrossed nicols)

with a fibrous fringe or as microcrystalline aggregates. Measurement of the percentage area occupied by quartz in an albitized granite and by vug-infilling minerals in an albite rock has been performed on thin sections with an interactive image analyzer (Lapique *et al.* 1988). In both cases, the percentage areas average 25% of the total surface. Vugs are generally irregular in shape and interconnected by narrow channelways along grain boundaries (Fig. 4). If some vugs (such as in deposit 225) remain empty and are outlined by well-terminated albite crystals, most vugs are filled by hydrothermal minerals. The crystal infills are euhedral or in rosettes, indicating growth in an open space. Microfractures coated with alkali feldspar or muscovite and cracks flanked by a clear albite rim within chessboard albite are often present.

In the 225 deposit, thin and closely spaced concentric cracks envelop some of the vugs (Fig. 5a). They are generally discontinuous and preferentially localized near the margins and within the albitic plagioclase. In one case, the cracks have been observed around the entire perimeter of a vug. Local intense brecciation of some chessboard albite along the vug walls (Fig. 5b) is probably related to these concentric cracks as both types of structures imply inflatening of the host rock or implosion of the vugs ('implosion breccia', Sibson 1986). These microstructures are sealed by quartz which is in optical continuity with that inside the vug. A few deformation structures (bent twins or shear fractures in plagioclase) are observed in albite rocks and are older than the vug infilling minerals. However, it is difficult to ascertain if they result from a submagmatic stage or if they are related to the albitization and vug-formation stages.

QUARTZ VEINLETS

Swarms of subparallel, quartz-dominated veinlets (Fig. 5c) are commonly developed in the albite zones. The density of veinlets is obviously higher within the central zones of albitization whereas veinlets are relatively uncommon outside the albitized zones. Veinlet swarms range from a few dm up to 1 m across and seldom extend for more than 20 m along strike, with 4–5 m as the common length. Their orientation varies from one site to another and within sites (Fig. 2).

Veinlets are mainly vertical or steeply dipping and define curved or concentric patterns (Figs. 3 and 6). Spacing of veinlets in a single swarm ranges from less than 1 mm to more than 10 cm as shown in the 152 deposit (Fig. 6) where the density of veinlets has been measured perpendicular to strike. Lastly, the main structures (albite zones, veinlet swarms, greisen-bordered veins) were cross-cut by cataclasic zones and fractures (Figs. 3 and 6).

Veinlets present a single or a dominant orientation at the metre-scale although two orientations are occasionally observed. Veinlets in a single swarm are strictly parallel. A few low-angle deviations from the main orientation may be observed at the thin section-scale, which originate from clear anisotropy of cross-cut minerals (e.g. fracture along albite cleavage). This principally occurs where the vein density is low.

Infilled vugs are cross-cut by the veinlets. However, on the basis of the similarity in nature and chemistry (except albite which is absent in the veinlets) of the vug- and veinlet-infilling minerals, both episodes are interpreted to have formed from a single, evolving fluid (Charoy & Pollard 1989). In places where vugs have remained empty, no veinlet development is observed. This would indicate that, locally, fluids were not available either for vug-infill or for veinlet formation.

The relative extension due to veinlet opening is variable in a single swarm, and depends somewhat on the scale of measurement. At the swarm-scale, 20 and 50% integrated extensions have been calculated for the two 3 m-wide cross-sections in the 152 site (Fig. 6) assuming an average width of 1 mm for each veinlet. An extension in the range 150–250% is common in the middle of veinlet swarms, although in one sample from the 171 site (Fig. 1) an extreme 568% extension was measured on a 3 cm long thin section. Minerals of the albite rocks that were repeatedly truncated are now highly elongated but the different fragments are neither laterally shifted nor deformed (Fig. 7). Whatever the finite extension, the surrounding albite rock is apparently not deformed. No dissolution or compressional structures (stylolites or solution features) are apparent in the field or in thin sections to accomodate the finite dilation due to the veinlet development.

In all deposits, vein infill mainly consists of a variable proportion of elongate crystals of quartz, K-feldspar and strongly zoned cassiterite; albite is typically lacking and fluorite is less common. Opening of the veinlets greatly elongated vug-filling minerals in a direction roughly normal to the orientation of the veinlets (Figs. 7 and 8b). The axis of elongation of the veinlet minerals and quartz *c*-axes are generally perpendicular (or inclined at $>80°$) to the vein walls. However, since the orientation of fibres may not be a good indicator of the opening direction of a vein (Cox 1987, Urai *et al.* 1991), the opening vector has been measured in three deposits (171, 207, 225 in Fig. 1) from the displacement of markers such as grain boundaries and twin planes in albite. The rose diagrams in Fig. 8(b) clearly shows that the veinlets are dilational, with an opening vector perpendicular to the veinlet walls.

Elongated crystals in veinlets usually contain thin slivers of wall rock and/or trails of two phase fluid inclusions that are parallel to the veinlet walls (e.g. Fig. 5d). Such features indicate a crack-seal process for veinlet opening (Ramsay 1980), involving repeated fracturing of the veinlet–wall interfaces with incremental growth of the veinlet filling material (antitaxial vein growth, Ramsay & Huber 1983). Width of the individual veinlets was measured on numerous thin sections from different deposits. The resulting histograms (Fig. 8a) are asymmetrical and show a maximum at approximately 20 μm which is similar to the width between successive sliver trails of the veinlet walls (crack–seal spacing). This

indicates that veinlets were made by the repeated addition of 20 μm-wide increments of new material.

The internal structure of the veinlet is partly depending on the mineral nature of the veinlet walls. K-feldspar in the veinlet occurs preferentially in syntaxial overgrowth on albite of the host rock. Where veinlets cross-cut large quartz crystals in albitized granite, the vein infill is composed of quartz with the same crystallographic orientation. Where veinlets cross-cut albite or a fine-grained mixture of newly formed albite and quartz (albite is lacking as veinlet material), the veinlet infill may be composed of stretched quartz crystals (Durney & Ramsay 1973, Cox & Etheridge 1983) or of quartz fibres with straight edges (Fig. 5d). Quartz fibres often exhibit irregular and sutured boundaries, undulose extinction and subgrain development, all microstructural features which are developed neither in quartz of the adjacent albitized granite nor in quartz infilling vugs of the host albite rock. This would suggest more likely a growth origin for these peculiar features although they usually correspond to deformation structures (McLaren & Hobbs 1972).

FLUID-INCLUSION CONSTRAINTS

A fluid-inclusion investigation has been performed on quartz and fluorite from albite rocks (vug and crack–seal veinlet) and from greisen-bordered veins in order to constrain P, T parameters and fluid composition (Pollard 1984, Charoy & Pollard 1989). No representative fluid inclusions contemporaneous with albitization and quartz dissolution events were found. Mainly two types of fluids, represented by multiphase and two phase inclusions were encountered in both types of hydrothermal alteration.

(1) Multiphase inclusions with halite (±sylvite) are present in vug-filling minerals in albite rocks. They homogenize by halite disappearance along a large temperature range corresponding to 30–44 wt% equivalent NaCl, whereas fluid homogenization by vapour disappearance occurs only over a restricted temperature range (the nearly vertical trend in the Fig. 9a). There is no counterpart on the opposite side of the L+V+H equilibrium curve. Inclusions of this type represent a fluid trapped under P–T conditions exceeding those of the solubility curve in the NaCl–H_2O system, in the L+H stability field. This signifies an heterogeneous trapping of a saturated fluid together with a variable amount of halite (Ramboz *et al.* 1982). The minimum salinity of this fluid would be at the intersection of this vertical trend with the L+V+H equilibrium curve for $T_{m\,NaCl} = T_H \approx 100°C$ (27 wt% eq. NaCl). Oversaturated fluids are also present in quartz and fluorite from greisen-bordered veins. However, plots in the Fig. 9(a) sharply contrasts with the former. If many multiphase inclusions plot along (or close to) the L+V+H equilibrium curve ($T_{m\,NaCl} = T_H \approx 350°C$, salinity average of 42 wt% eq. NaCl), there is a large scatter of data on both sides of the equilibrium curve. This suggests the heterogeneous trapping of either halite or vapour from a saturated boiling fluid (Fig. 9b). Evidence of boiling was encountered in one greisen sample which would suggest an hydrostatic pressure around 100 bars. More diluted fluids (≈30 wt% eq. NaCl) were trapped along the L+V+H equilibrium curve at lower temperatures (Fig. 9a).

The minimum trapping pressure of inclusions homogenizing by halite disappearance cannot be estimated directly. The minimum possible pressure of trapping will be the pressure at the temperature of halite disappearance. The occurrence of saturated high temperature fluids in the L+H stability field commonly precludes any shallow level of trapping (Sourirajan & Kennedy 1962). Higher temperatures of halite disappearance relate primarily to greater NaCl concentrations rather than to higher pressure. Inclusions in vug-filling fluorite of albite rocks which could not have been boiling therefore require minimum pressure of about 190 bars (Sourirajan & Kennedy 1962).

(2) Results concerning two-phase inclusions in albite rocks and greisen-bordered veins are presented as histograms in Fig. 10(a). More significant to the present discussion are the maxima between 360 and 420°C which represent a major fluid influx during both mineralizing hydrothermal episodes. Two-phase inclusions trapped during sealing of the crack-seal process in trails parallel to the quartz-veinlet walls in albite rocks are presumably primary or pseudo-secondary. They exhibit a variable salinity (3–18 wt% eq. NaCl) and homogenize either to liquid or vapour in the 300–400°C range, with a few inclusions showing a critical behaviour around 400°C (≈4 wt% eq. NaCl), for 285 bars of hydrostatic pressure (Fig. 10b). Some inclusions homogenize by liquid disappearance at temperatures close to 500°C which seems to reflect necking-down or leakage of inclusions during the sealing process. Two-phase inclusions in greisen-bordered veins are secondary with respect to multiphase inclusions but appear primary in quartz, fluorite and cassiterite. Salinity is in the range 4–9 wt% eq. NaCl. They also homogenize to liquid or vapour in the same range of temperature as those in the crack–seal veinlets (Fig. 10a), which would indicate that fluid was trapped close to critical conditions. Some inclusions contain sufficient CO_2 in the vapour phase to nucleate clathrate during freezing runs. Pure liquid CO_2 as a separate component is very uncommon. Salinity is in the range 4–9 wt% eq. NaCl.

A reconnaissance oxygen isotope study was undertaken on granite, albite rock and vug-filling minerals. The lowering of an initial $\delta^{18}O$ for whole-rock unaltered granite from 7.8 to 9.8‰ down to an average of 6.7‰ for albite rock was interpreted by Pollard *et al.* (1990) as the result of intensive interaction with external meteoric waters. However, there is no simple relationship between calculated $\delta^{18}O$ of the fluid from fluid inclusion data. A simple mixing mechanism between early, high salinity, magmatic fluids ($\delta^{18}O$ from 6 to 10‰) with low salinity, colder meteoric fluids ($\delta^{18}O \approx -15‰$), is not clearly constrained because of the absence of more

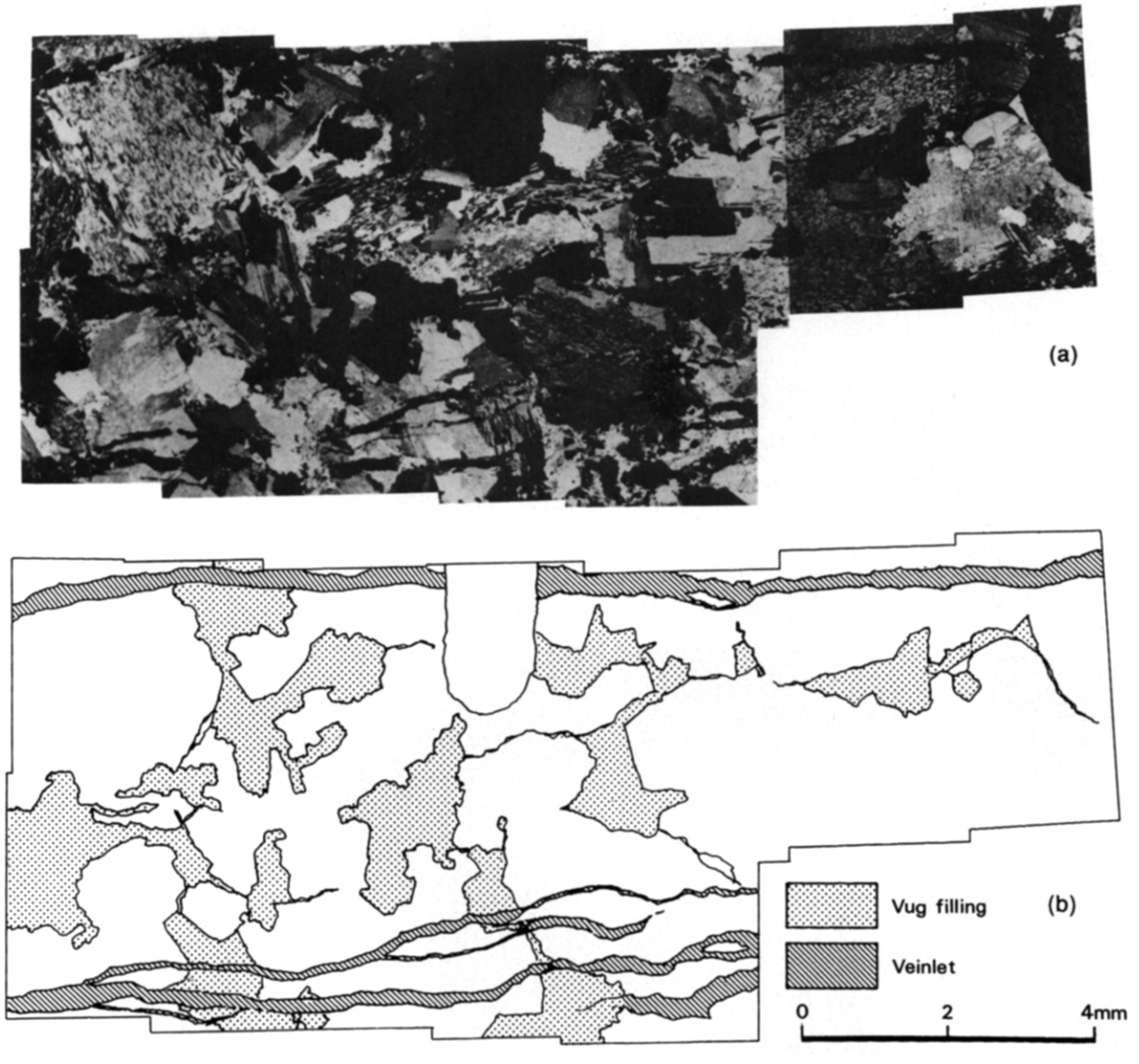

Fig. 4. (a) Assemblage of microphotographs under crossed nicols and (b) drawing of a thin section (207 deposit) showing channelways between the vugs (dotted area) which predate the veinlets (hatched area). The veinlets are filled with quartz, fluorite, K-feldspar and cassiterite.

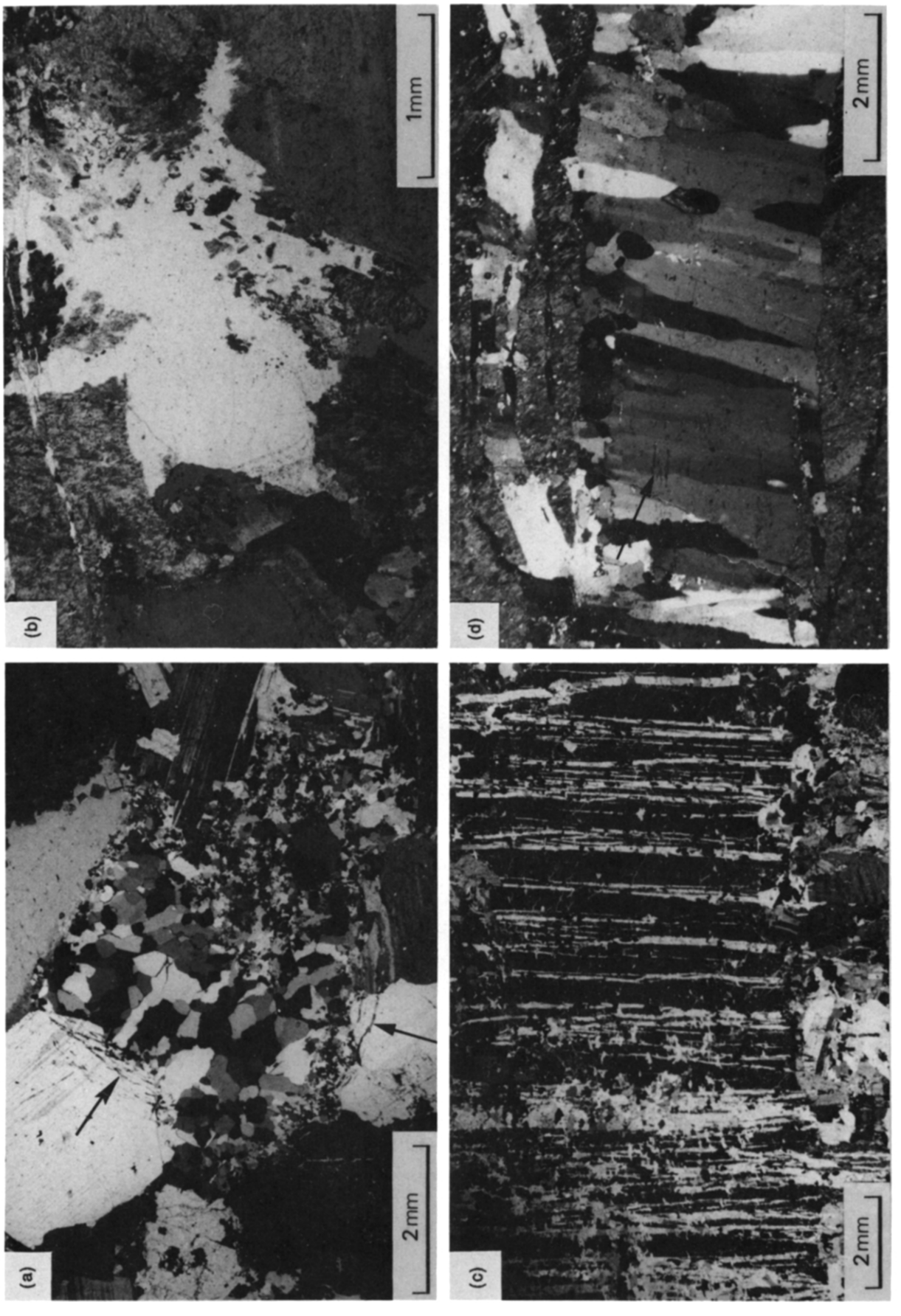

Fig. 5. Photomicrographs of thin sections (crossed nicols). (a) Concentric microcracks (arrows) in albite around a vug; these microcracks are filled by quartz that is in optical continuity with the vug infill. (b) Vug with fragments of albite and chessboard albite. Note the small horizontal veinlet which cross-cuts the vug in the upper part of the photomicrograph. (c) Thin quartz veinlets cross-cutting a chessboard albite. Extension is 31% parallel to length of picture. (d) Internal structure of a veinlet showing the quartz fibres at high angle to the vein walls and the thin inclusion bands (arrow) parallel to the vein walls. Note the small diverging veinlet in the upper part of the photomicrograph.

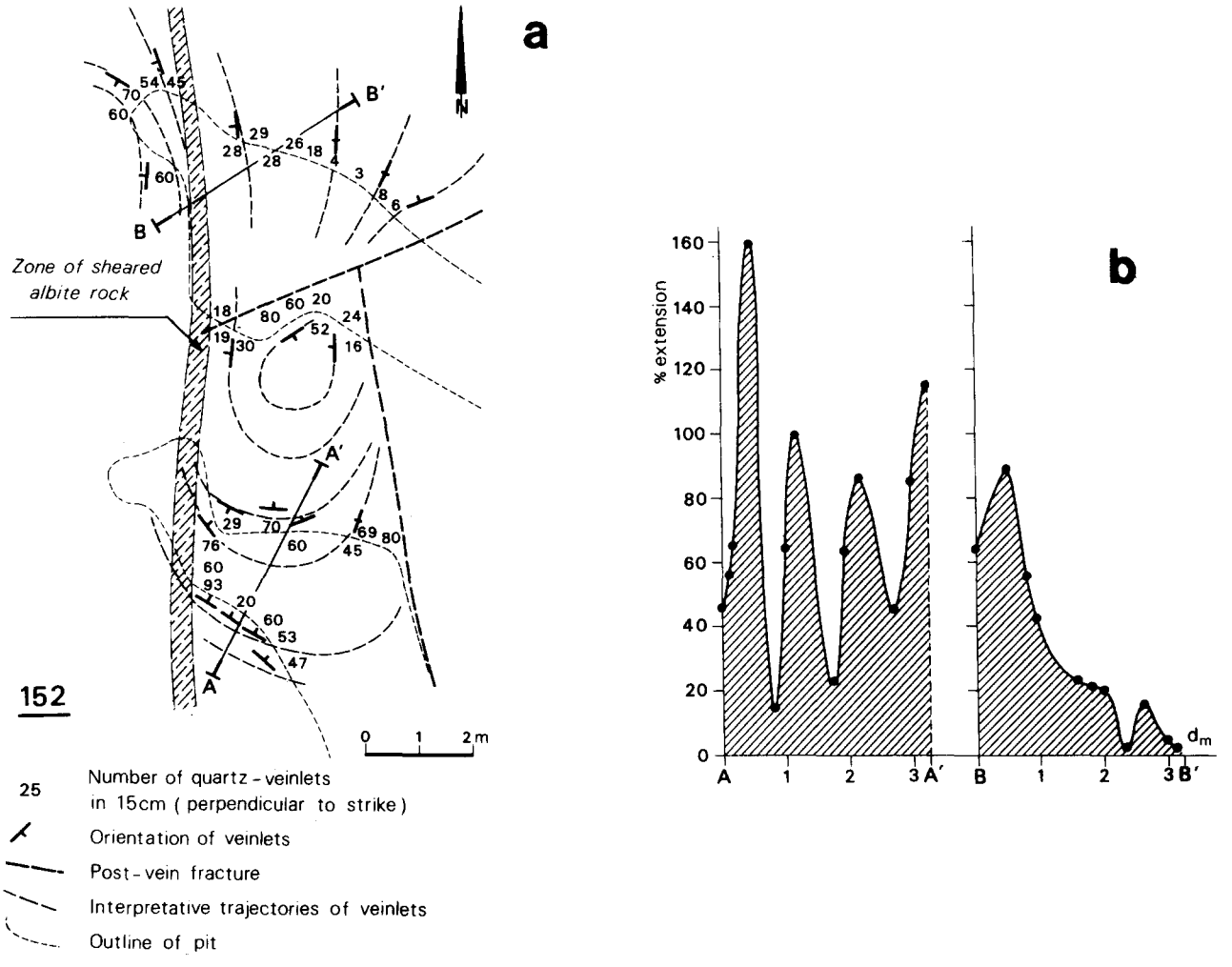

Fig. 6. (a) Map of the 152 deposit showing the density and orientations of veinlets in the albite rock. (b) Diagrams showing the extension across the two profiles AA′ and BB′ in (a); the extension has been calculated from the density of veinlets and assuming a 1 mm width for each veinlet.

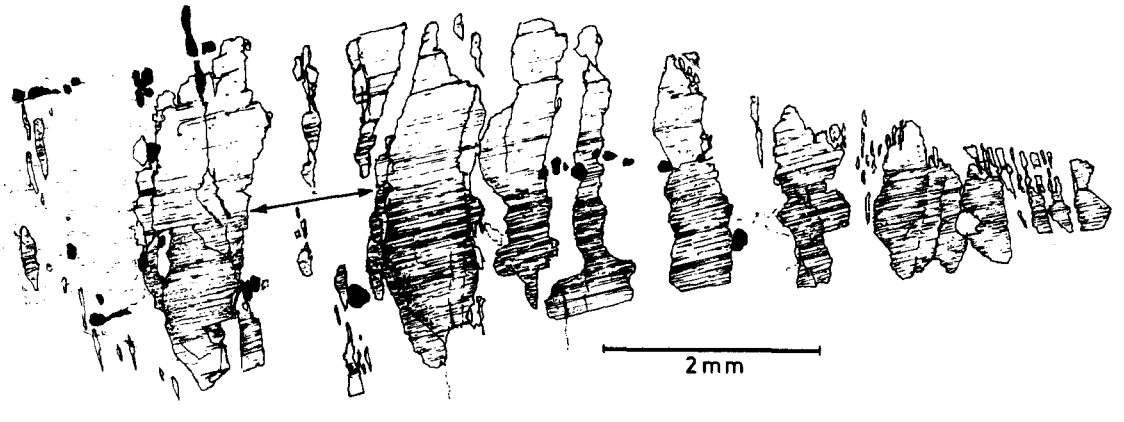

Fig. 7. Drawing of a fractured albite crystal offset by quartz veinlets (225 deposit). The arrow indicates the opening vector as determined by the displacement of twins. Quartz fibres in the veinlets are parallel to that vector and not strictly perpendicular to the vein wall. Elongation is 68%. Black: cassiterite crystals.

detailed and representative data on mineral separates and of the complex history of the telescoped fluid interactions in space and time.

Although pressures, temperatures and fluid/rock ratios calculated or estimated above remain badly constrained, fluid inclusion investigations have shown that the fluids leading to vug- and veinlet-filling and to greisenization of the Emuford granite do have similar compositions. However, it appears that they are in different physical states: if the former are in the L+H state, the latter are in the L+V+H state. Such a difference may govern the nature of the precipitated minerals, the mode of circulation of the fluids and their penetrativity into the host rocks.

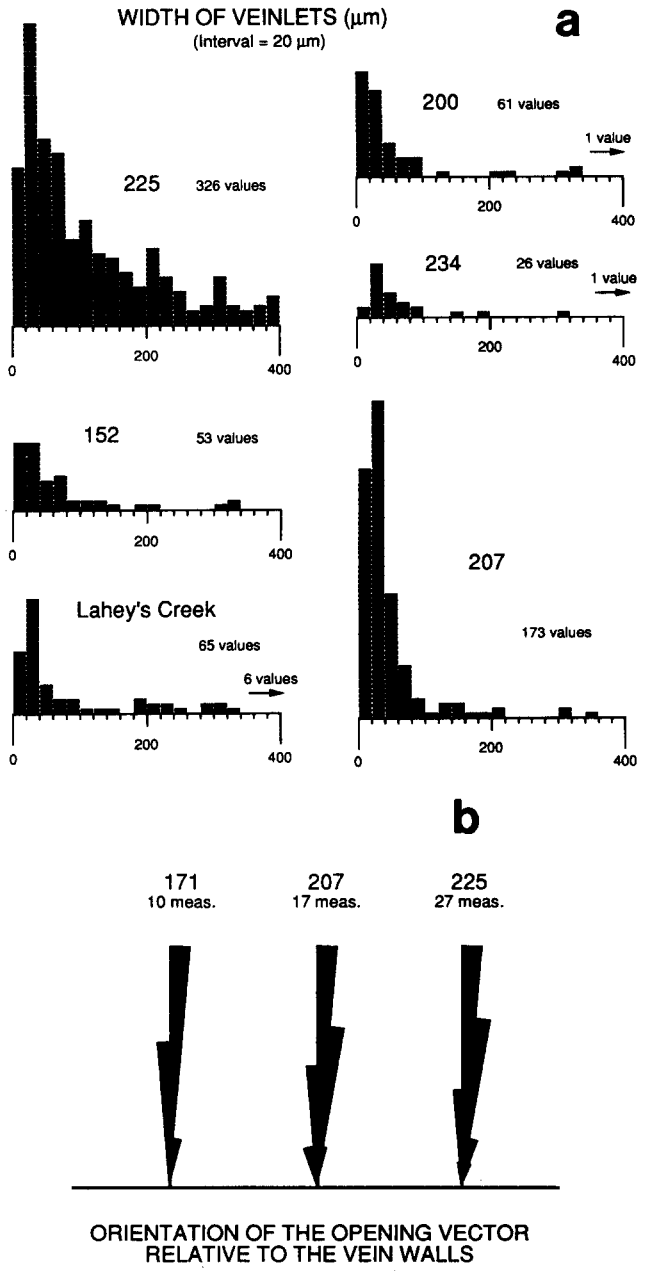

Fig. 8. Geometrical characteristics of quartz veinlets in samples from several deposits. (a) Histograms of veinlet widths. (b) Rose diagrams of the opening directions (5° angle classes).

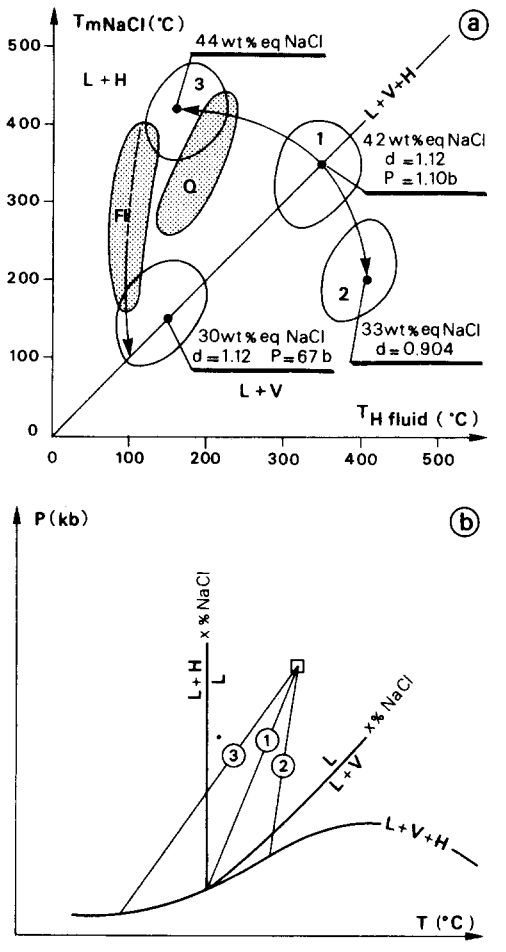

Fig. 9. (a) $T_{m\ NaCl}$ (halite dissolution) vs $T_{H\ fluid}$ (vapour bubble disappearance) for multiphase inclusions in fluorite and quartz from albite rocks (stippled) and greisens; explanation of (1), (2) and (3) in (b). (b) Trapping conditions and isobaric behaviour of multiphase inclusions in the H_2O–NaCl system: (1) L+V+H equilibrium; (2) L → L+V → L+V+H; and (3) L → L+H → L+H+V; only the cooling path (1) is isochoric.

INTERPRETATION AND DISCUSSION

From the former mineralogical and structural features, the following interpretative sequence of events in the albitized zones is proposed (Fig. 11).

First stage

During cooling of the Emuford pluton, the hydrothermal fluid activity was concentrated around small high-level, late-stage intrusions and consisted in local convection cells. A stock can create its own aureole of permeability rather than being dependent only upon externally applied shear couples to produce permeability. Hot ascending Na- and F-rich fluids of magmatic origin contributed to the disappearance of biotite and the transformation of alkali feldspar into chessboard albite to form albitized granite. Percolation of these fluids was probably diffuse and localized by grain boundaries. They initially promoted the coarsening of perthite exsolution (Na–K exchange by diffusion). Alkali feldspar may have a porosity at the micron-scale as high as 4.5% (Worden *et al.* 1990) which may facilitate diffusional transport. Alkali feldspars represent on modal average 38% of the granite (Pollard 1984) and constitute a continuous framework contributing to a global porosity of 1–2% in the unaltered granite before albitization. Under a triaxial stress system, fluids tend to migrate along the planes under tension, that is, normal to the minimum principal stress. Microfractures, cleavage or twin planes, and crystal boundaries oriented in such a direction provide preferential channelways. The rough NW–SE orientation of the majority of the albite zones (Fig. 2) may be interpreted in terms of preferential percolation, perpendicular to the minimum compressive regional stress σ_3, deduced from the statistical average strike of the contemporaneous quartz–tourmaline and quartz–chlorite vein swarms in the surrounding metamorphics (Fig. 2).

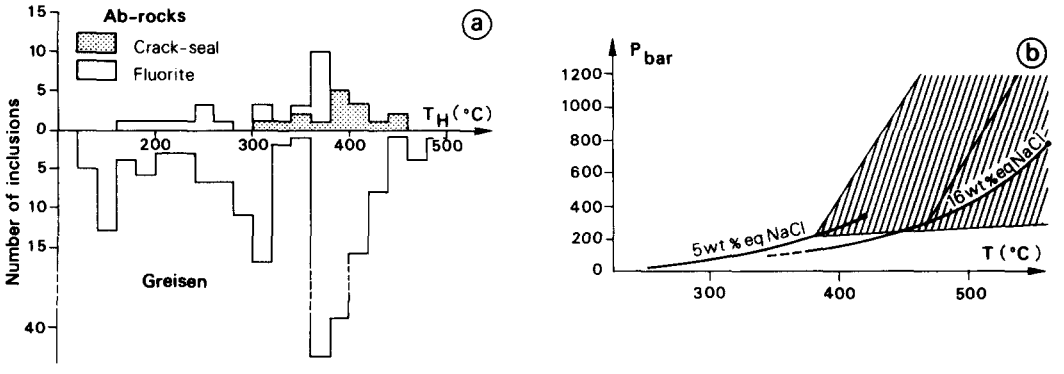

Fig. 10. (a) Histograms of homogenization temperatures of the two-phase inclusions in albite rocks (upper) and greisens (lower). (b) *P–T* diagram showing the possible conditions for trapping of the two-phase inclusions (hatched area). The two L+V curves correspond to different values of salinity.

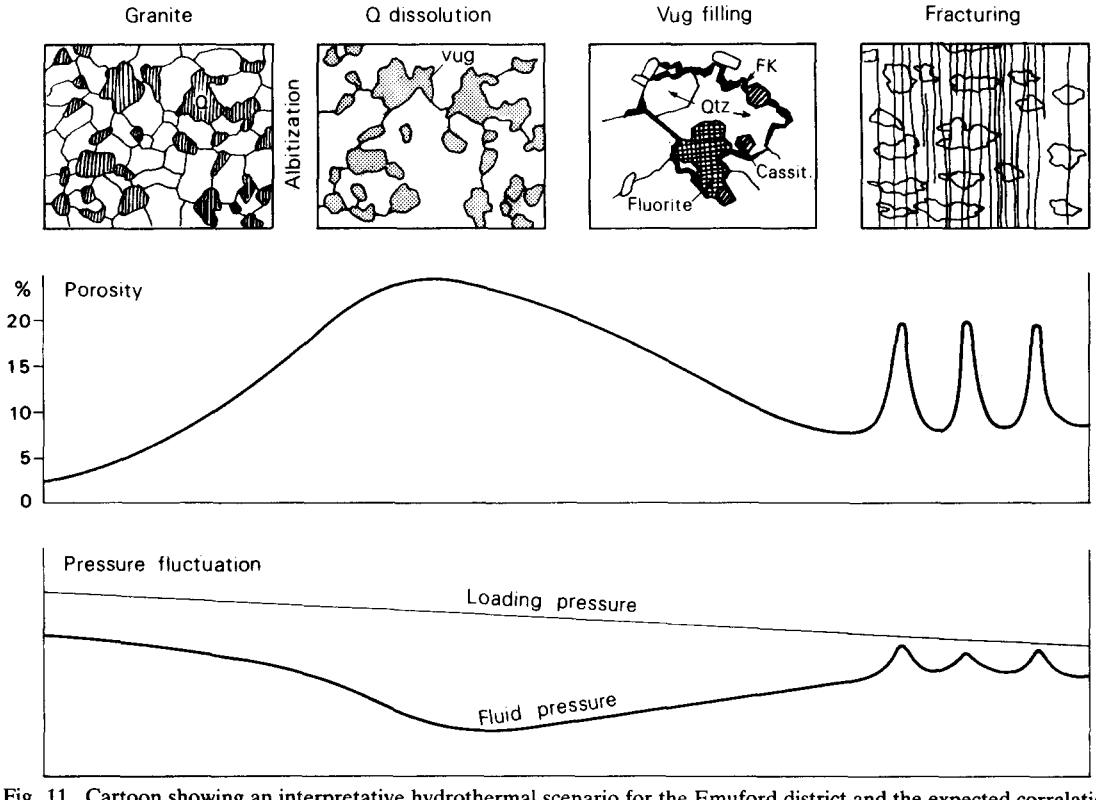

Fig. 11. Cartoon showing an interpretative hydrothermal scenario for the Emuford district and the expected correlation between textures and qualitative estimates of permeability and fluid pressure variability. The decreasing slope of the load pressure is attributed to the erosion above the pluton.

Second stage

The albitization process resulted in the K-enrichment of the percolating fluids which became more aggressive with respect to quartz, with the consequent dissolution of the initial granite quartz and the formation of the vuggy albite rock. This contributed to a considerable increase in porosity (interconnected vugs) which was sufficient to allow a Darcian flow style for fluid circulation. Such a large increase of permeability (chemically-controlled permeability) caused by quartz removal led to the lowering of pressure which is consistent with the observed brecciation of the chessboard albite (brittle behaviour) and development of local concentric cracks that we interpret as equivalent to implosion breccia around vugs. This would suggest that the difference between local grain-scale σ_3 and the fluid pressure in the vug was sufficiently high to cause spalling of the surrounding minerals. Contrary to other cases of quartz dissolution (episyenitization) from the literature (Cheilletz & Guiliani 1982, Lespinasse 1984, Cathelineau 1987), no deformation at the pluton scale occurred during these two first hydrothermal events which therefore are assumed to have been isovolumic and static processes.

Third stage

The suspected decrease of fluid pressure promoted the downward influx of external (meteoric) fluids resulting in the cooling and dilution of the former magmatic brines. These external fluids were preferentially drained into the highly porous albite rocks which were favourable loci for their accumulation. Infill of most of the vugs

by a complex sequence of hydrothermal minerals would be the result of this large input of external fluids. The significant drop in salinity would cause the decrease in silica solubility (Fournier 1955) and quartz is then the main mineral to precipitate in the vugs. Consequently, the fluid pressure progressively increased as the consequence of the sealing of most of the vugs and channelways.

Fourth stage

The generation of the veinlet swarms is interpreted as a direct consequence of the increasing fluid pressure induced by the former decreasing porosity (Walder & Nur 1984). This assumption is supported by the fact that where vugs remain empty, no veinlet development is observed. Since permeability at grain boundary was no longer sufficient to permit fluid circulation, a secondary permeability was mechanically induced, and fracturing through the mechanically weakened albite rocks was driven to release fluid pressure excess. The fluid flow could then become non-Darcian or turbulent. Hydraulic fracturing occurred normal to the minimum compressive stress σ_3 and for low values of $\sigma_1-\sigma_3$ (Secor 1965). However, the concentric pattern of veinlet orientations in the pits (Figs. 3 and 6) indicates that high pressure cells probably existed at a decametric scale. These patterns may be compared with the calculated stress field around a granitic body and with the expected $\sigma_1-\sigma_3$ trajectories on top of a pressure cell (Anderson 1936, Roberts 1970, Moore 1975).

The absence of dissolution (volume loss), transformation (wall-rock alteration) or deformation features in the wall rocks signifies that the veinlet growth was not due to dissolution–recrystallization processes but resulted from pure dilation by repeated short-lived opening and sealing processes with new material deposited from circulating fluids.

CONCLUSIONS

The well-established sequence of telescoped alteration–mineralization features, together with the different styles of porosity and the changes in the induced permeability during evolution of the albitized zones and associated veinlet swarms at Emuford reflect variation in mode of fluid flow rather than variation in fluid composition during cooling of the pluton. Charoy & Pollard (1989) suggested that albitization and quartz dissolution were closely linked, with increasing quartz solubility resulting from potassium enrichment in the fluid phase during albitization. The large increase in permeability caused by quartz dissolution has to lower the ambient pressure and to increase the fluid alkalinity. Consequently, albitization and quartz dissolution may be considered as self-accelerated alteration processes. An important consequence of this dramatic increase in permeability in space and time will be an introduction of heterogeneity in the cooling rate of the pluton and the consequent pumping out of large volumes of external fluids into a very restricted volume of rock. In this respect, they contrast with greisen zones which appear to result from widespread large-scale fracture development and intensive chemical exchange between the fluid and the surrounding rocks (Charoy 1979). In both type of alteration zones, factors such as permeability, fluid pressure, physical state of the fluids and style of fluid flow are the most important parameters in producing the contrasting styles of mineralization rather than large differences in fluid composition. No early fracturing was developed in the albite zones and pressure reduction is supposed to have been produced by quartz dissolution and increase in permeability. The introduction of meteoric fluids resulted in dilution and induced silica saturation in the high-salinity fluid, leading to precipitation of quartz and other hydrothermal minerals in vugs. Rising fluid pressure (to near lithostatic values) was caused by decreasing permeability and resulted in development of crack–seal veins localized within the previously albitized, and therefore brittle, zones. The initiation and development of the veinlet systems indicate that fluids accumulated locally and caused their extension hydraulically. Fibre veins crystallized when the fluid pressure was maintained close to the level required for hydraulic fracturing.

The scenario presented in this study results, for the main part, from a careful identification of fine-scale textural features. The sequence of events displayed at a few localities in the Emu Suite granites was constrained by the relations in time and space of the new minerals growing during the overprinting episodes of alteration. It is emphasized that detailed textural study may be of particular importance in understanding the physical parameters prevailing during hydrothermal alteration of magmatic bodies.

Acknowledgements—The authors are grateful to Steve F. Cox and an anonymous reviewer for a critical and constructive review of the paper. They thank Ken Lawrie and Jean Macaudière for comments on an earlier version of the manuscript and Y. Lestreit for the drawings. C.R.P.G. contribution number 1044.

REFERENCES

Anderson, E. M. 1936. The dynamics of the formation of cone-sheets, ring-dykes and cauldron subsidences. *Proc. R. Soc. Edinburgh* **56**, 128–163.

Blake, D. H. & Smith, J. W. 1970. Mineralogical zoning in the Herberton tinfield, north Queensland, Australia. *Econ. Geol.* **65**, 993–997.

Boullier, A. M. & Robert, F. 1992. Paleoseismic events recorded in Archaean gold–quartz vein networks, Val d'Or, Abitibi, Quebec. *J. Struct. Geol.* **14**, 161–179.

Brimhall, G. H., Jr. 1977. Early fracture-controlled disseminated mineralization at Butte, Montana. *Econ. Geol.* **72**, 37–59.

Burnham, C. W. 1979. Magmas and hydrothermal fluids. In: *Geochemistry of Hydrothermal Ore Deposits* (2nd edn) (edited by Barnes, H. L.), 71–135.

Burt, D. M. 1981. Acidity–salinity diagrams. Application to greisen and porphyry deposits. *Econ. Geol.* **76**, 832–843.

Cathelineau, M. 1987. Les interactions entre fluides et roches: thermométrie et modélisation. Unpublished Thèse Doct., I.N.P.L. Nancy.

Cathelineau, M., Boiron, M. C., Essaraj, S., Dubessy, J., Lespinasse, M. & Poty, B. 1993. Fluid pressure variations in relation to multistage deformation and uplift: a fluid inclusion study of Au quartz veins. *Eur. J. Mineral.* **5**, 107–121.

Charoy, B. 1979. Définition et importance des phénomènes deutériques et des fluides associés dans les granites. Conséquences métallogéniques. Thèse d'Etat. *Mém. Sci. de la Terre* **37**.

Charoy, B. & Pollard, P. J. 1989. Albite-rich, silica-depleted metasomatic rocks at Emuford, northeast Queensland: mineralogical, geochemical and fluid inclusion constraints on hydrothermal evolution and tin mineralization. *Econ. Geol.* **84**, 1850–1874.

Cheilletz, A. & Giuliani, G. 1982. Rôle de la déformation des granites dans la genèse des épisyénites feldspathiques des massifs de Lovios-Geres (Galice) et des Zaër (Maroc central). Relations avec les minéralisations en tungstène-étain associées. *Mineral. Deposita* **17**, 387–400.

Coney, P. J., Edwards, A., Hine, R., Morrison, F. & Windrim, D. 1990. The regional tectonics of the Tasman orogenic system, eastern Australia. *J. Struct. Geol.* **12**, 519–543.

Cox, S. F. 1987. Antitaxial crack-seal vein microstructures and their relationship to displacement paths. *J. Struct. Geol.* **9**, 779–787.

Cox, S. F. 1991. Geometry and internal structures of mesothermal vein systems: implications for hydrodynamics and ore genesis during deformation. In: *Structural Geology in Mining and Exploration. Extended Abstracts. Univ. West. Aust. Publ.* **25**, 47–53.

Cox, S. F. & Etheridge, M. A. 1983. Crack-seal fibre growth mechanisms and their significance in the development of oriented layer silicate microstructures. *Tectonophysics* **92**, 147–170.

Cox, S. F., Etheridge, M. A. & Wall, V. J. 1986. The role of fluids in syntectonic mass-transport, and the localization of metamorphic vein-type ore deposits. *Ore Geol. Rev.* **2**, 65–86.

Cox, S. F., Wall, V. J., Etheridge, M. A. & Potter, T. F. 1991. Deformational and metamorphic processes in the formation of mesothermal vein-hosted gold-deposits. Examples from the Lachlan fold belt in central Victoria, Australia. *Ore Geol. Rev.* **6**, 391–423.

Durney, D. W. & Ramsay, J. G. 1973. Incremental strains measured by syntectonic crystal growth. In: *Gravity and Tectonics* (edited by De Jong, K. A. & Scholten, R.). Wiley, New York, 67–96.

Etheridge, M. A., Cox, S. F., Wall, V. J. & Vernon, R. H. 1984. High fluid pressures during regional metamorphism and deformation: implications for mass-transport and deformation mechanisms. *J. geophys. Res.* **86**, 4344–4358.

Fournier, R. O. 1985. The behaviour of silica in hydrothermal solutions. In: *Geology and Geochemistry of Epithermal Deposits* (edited by Berger, B. R. & Bethke, P. M.). *Rev. Econ. Geol.* **2**, 45–62.

Fyfe, W. S., Price, N. J. & Thompson, A. B. 1978. *Fluids in the Earth's Crust*. Elsevier, Amsterdam.

Guilbert, J. M. & Park, C. F., Jr. 1986. *The Geology of Ore Deposits*. Freeman, New York.

Hemley, J. J., Montoya, J. W., Marinenko, J. W. & Luce, R. W., 1980. Equilibria in the system. Al_2O_3–SiO_2–H_2O and some general implications for alteration/mineralization processes. *Econ. Geol.* **75**, 210–228.

Lapique, F., Champenois, M. & Cheilletz, A. 1988. Un analyseur vidéographique interactif: description et applications. *Bull. Minéral.* **111**, 679–687.

Lespinasse, M. 1984. Contexte structural des gisements d'uranium de la Marche occidentale; fracturation, circulations fluides, propagation de l'épisyénitisation. *Mem. Géol. Géochim. Uranium* **8**.

McLaren, A. C. & Hobbs, B. E. 1972. Transmission electron microscope investigation of some naturally deformed quartzites. In: *Flow and Fracture of Rocks* (edited by Heard, H. C., Borg, I. Y., Carter, N. L. & Raleigh, C. B.). *Am. geophys. Un. Geophys. Monogr.* **16**, 55–66.

Moore, J. McM. 1975. A mechanical interpretation of the vein and dyke systems of the S.W. England orefield. *Mineral. Deposita* **10**, 374–388.

Moore, D. E. & Liou, J. G. 1979. Chessboard-twinned albite from Franciscan metaconglomerates of the Diablo range, California. *Am. Miner.* **64**, 329–336.

Norton, D. & Knapp, R. 1977. Transport phenomena in hydrothermal systems: the nature of porosity. *Am. J. Sci.* **277**, 913–936.

Norton, D. & Knight, J. 1977. Transport phenomena in hydrothermal systems: cooling plutons. *Am. J. Sci.* **277**, 937–981.

Orville, P. M. 1963. Alkali ion exchange between vapour and feldspar phases. *Am. J. Sci.* **261**, 201–237.

Parsons, I., Rex, D. C., Guise, P. & Halliday, A. N. 1988. Argon-loss by alkali felspars. *Geochim. cosmochim. Acta* **52**, 1097–1112.

Peng, C. C. J. 1970. Intergranular albite in some granites and syenites of Hong Kong. *Am. Miner.* **55**, 270–282.

Pollard, P. J. 1984. Granites and associated tin–tungsten mineralization in the Emuford district, northeast Queensland, Australia. Unpublished Ph.D. dissertation, James Cook University, North Queensland, Australia.

Pollard, P. J. 1988. Petrogenesis of tin-bearing granites of the Emuford district, Herberton tinfield, northeast Queensland, Australia. *Aust. J. Earth Sci.* **35**, 39–57.

Pollard, P. J. & Taylor, R. G. 1986. Progressive evolution of alteration and tin mineralization: controls by interstitial permeability and fracture-related tapping of magmatic fluid reservoirs in tin granites. *Econ. Geol.* **81**, 1795–1800.

Pollard, P. J., Pichavant, M. & Charoy, B. 1987. Contrasting evolution of fluorine- and boron-rich tin systems. *Mineral. Deposita* **22**, 315–321.

Pollard, P. J., Golding, S. D., Witt, W. K., Milburn, D. & Taylor, R. G. 1990. Reconnaissance oxygen isotope study of tin-bearing granites and associated alteration/mineralization, Herberton tinfield, northeastern Queensland, Australia. In: *Stable Isotopes and Fluid Processes in Mineralization* (edited by Herbert, H. K. & Ho, S. E.). *Univ. West. Aust. Publ.* **23**, 324–332.

Ramberg, H. 1962. Intergranular precipitation of albite formed by unmixing of alkali feldspar. *Neues Jb. Miner. Abh.* **98**, 14–31.

Ramboz, C., Pichavant, M. & Weisbrod, A. 1982. Fluid immiscibility in natural processes: use and misuse of fluid inclusion data. II Interpretation of fluid inclusion data in terms of immiscibility. *Chem. Geol.* **37**, 29–48.

Ramsay, J. G. 1980. The crack-seal mechanism of rock deformation. *Nature* **284**, 135–139.

Ramsay, J. G. & Huber, M. I. 1983. *Modern Techniques of Structural Geology, Volume* 1: *Strain Analysis*. Academic Press, London.

Roberts, J. L. 1970. The intrusion of magmas into brittle rocks. In: *Mechanism of Igneous Intrusion* (edited by Newall, G. & Rast, N.). Gallery, London, 287–338.

Secor, D. T. 1965. Role of fluid pressure in jointing. *Am. J. Sci.* **263**, 633–646.

Sibson, R. H. 1986. Brecciation processes in fault zones: inferences from earthquake rupturing. *Pure & Appl. Geophys.* **124**, 159–175.

Sibson, R. H., Robert, F. & Poulsen, K. H. 1988. High angle reverse faults, fluid-pressure cycling and mesothermal gold–quartz deposits. *Geology* **16**, 551–555.

Smith, J. V. 1974. *Feldspar Minerals.* 2: *Chemical and Textural Properties*. Springer, New York.

Sourirajan, S. & Kennedy, G. C. 1962. The system H_2O–NaCl at elevated temperatures and pressures. *Am. J. Sci.* **260**, 115–141.

Titley, S. R. 1990. Evolution and style of fracture permeability in intrusive-centered hydrothermal systems. In: *The Role of Fluids in Crustal Processes; Studies in Geophysics*. National Research Council. National Academic Press, Washington, DC, 50–63.

Urai, J. L., Williams, P. F. & Van Roermund, H. L. M. 1991. Kinematics of crystal growth in syntectonic fibrous veins. *J. Struct. Geol.* **13**, 823–836.

Walder, J. & Nur, A. 1984. Porosity reduction and crustal pore pressure development. *J. geophys. Res.* **89**, 11,539–11,548.

Worden, R. H., Walker, D. L., Parsons, I. & Brown, W. L. 1990. Development of microporosity, diffusion channels and deuteric coarsening in perthitic alkali feldspars. *Contr. Miner. Petrol.* **140**, 507–515.